



저작자표시-비영리-변경금지 2.0 대한민국

이용자는 아래의 조건을 따르는 경우에 한하여 자유롭게

- 이 저작물을 복제, 배포, 전송, 전시, 공연 및 방송할 수 있습니다.

다음과 같은 조건을 따라야 합니다:



저작자표시. 귀하는 원저작자를 표시하여야 합니다.



비영리. 귀하는 이 저작물을 영리 목적으로 이용할 수 없습니다.



변경금지. 귀하는 이 저작물을 개작, 변형 또는 가공할 수 없습니다.

- 귀하는, 이 저작물의 재이용이나 배포의 경우, 이 저작물에 적용된 이용허락조건을 명확하게 나타내어야 합니다.
- 저작권자로부터 별도의 허가를 받으면 이러한 조건들은 적용되지 않습니다.

저작권법에 따른 이용자의 권리는 위의 내용에 의하여 영향을 받지 않습니다.

이것은 [이용허락규약\(Legal Code\)](#)을 이해하기 쉽게 요약한 것입니다.

[Disclaimer](#)

박 사 학 위 논 문

GLDC Promotes Cisplatin Resistance of Ovarian Cancer Cells by Enhancing mtROS-Driven Mitochondrial Fission

계 명 대 학 교 대 학 원
의 학 과

D O T H I Y E N

GLDC Promotes Cisplatin Resistance of Ovarian Cancer Cells by
Enhancing mtROS-Driven Mitochondrial Fission

Do
Thi
Yen

지 도 교 수 신 소 진

2
0
2
5
년
2
월

2 0 2 5 년 2 월

GLDC Promotes Cisplatin Resistance of Ovarian Cancer Cells by Enhancing mtROS-Driven Mitochondrial Fission

지도교수 신 소 진

이 논문을 박사학위 논문으로 제출함

2025년 02월

계명대학교 대학원

의학과 산부인과학 전공

D O T H I Y E N

DO THI YEN의 박사학위 논문을 인준함

주 심 서 지 혜

부 심 신 소 진

부 심 하 은 영

부 심 김 진 영

부 심 송 권 호

계 명 대 학 교 대 학 원

2 0 2 5 년 2 월

Table of Contents

1. Introduction	1
2. Materials and Methods	2
3. Results	11
4. Discussion	37
5. Summary	39
References	40
Abstract	45
국문초록	47

List of Figures

Figure 1. Analysis of GLDC gene expression in cancers	18
Figure 2. Survival analysis of GLDC in patients with ovarian cancer	20
Figure 3. Scheme of establishment of CP-resistant ovarian cancer cells in an <i>in vitro</i> model	21
Figure 4. Cytotoxic effect of CP on resistant and parental ovarian cancer cells in an <i>in vitro</i> model	22
Figure 5. Scheme of an <i>in vivo</i> experiment to evaluate the cytotoxic effect of CP on ovarian cancer	23
Figure 6. Cytotoxic effect of CP on ovarian cancer cells in an <i>in vivo</i> model	24
Figure 7. Analysis of GLDC expression in CP-resistant ovarian cancer cells	25
Figure 8. Analysis of knockdown GLDC in CP-resistant ovarian cancer cells	26
Figure 9. Analysis of GLDC function in CP resistance across various	

types of ovarian cancer cells	27
Figure 10. Analysis of relative mtROS level in ovarian cancer cells ...	28
Figure 11. Synergistic effect of MT on CP-resistant ovarian cancer cells	29
Figure 12. Analysis of mitochondrial fission in CP-resistant ovarian cancer cells	30
Figure 13. Analysis of mtROS-induced mitochondrial fission using Mdivi-1 treatment in CP-resistant ovarian cancer cells	32
Figure 14. Analysis of PKC δ -induced mitochondrial fission in ovarian cancer cells	34
Figure 15. Analysis of mtROS-driven PKC δ phosphorylation using B106 treatment in CP-resistant ovarian cancer cells	35
Figure 16. Schematic illustration of the main results of this study	36

List of Tables

Table 1. Antibodies Used for Western Blotting 9

Table 2. Primer Pair Sequences Used for RT-PCR 10

1. Introduction

Ovarian cancer (OC) currently remains the fatal mortality in women worldwide (1). Over the past two decades, combination chemotherapy, including cisplatin (CP), has improved the overall survival rates of patients with advanced OC (2–4). However, despite optimal surgery and appropriate first-line chemotherapy, approximately 70% of patients with OC experience recurrence at different time points (5). The goal of sequential chemotherapy for recurrent ovarian cancer is to maximize therapeutic benefits while minimizing toxicity, however, this approach is not curative, suggesting a severe chemoresistant problem (6). The high rate of chemoresistance emphasize the major challenge in OC treatment, thereby highlighting the unmet need to develop new drug or strategies to overcome chemoresistance in OC.

Glycine decarboxylase (GLDC) is a primary enzyme in the glycine cleavage system. GLDC catalyzes the cleavage of glycine, and then transfers a one-carbon moiety to tetrahydrofolate (THF) while releasing carbon dioxide (CO₂). GLDC serves as a hallmark regulator of the glycine metabolic pathway (7). Previous studies have demonstrated that elevated expression of GLDC drives the tumorigenic capacity in non-small cell lung cancer (NSCLC) (8), neuroblastoma (9), and hepatocellular carcinoma (HCC) (10). These findings indicate that GLDC is a promising target in the development of cancer therapies. However, the biological role of GLDC in OC remains unexplored, particularly in the context of chemoresistance. Further investigation is required to elucidate the underlined mechanism of GLDC-induced adaptation in OC cells to chemotherapy.

2. Materials and Methods

2.1. Gene expression and clinical outcome analysis:

The mRNA expression levels of GLDC in different types of cancer was obtained from TNMplot.com (<http://tnmplot.com/analysis>). TNMplot.com is a well-known platform designed for analyzing gene expression data from normal and tumor tissues across different cancer types (11). In this study, the expression level of GLDC were analyzed across the ten most common cancers in women, using RNASeq data from 56,938 samples obtained from Gene Expression Omnibus (GEO) and The Cancer Genome Atlas (TCGA) databases. The diagrams were generated to visually represent the mRNA expression level of GLDC in OC tissues compared to normal ovary tissues. The p value was analyzed using the Mann-Whitney test.

The gene expression of GLDC according to OC stages was analyzed using Gene Expression Profiling Interactive Analysis (GEIPA) web server (<http://gepia.cancer-pku.cn/index.html>). The GEIPA platform was reported as an online database for analyzing the gene expression profiling of tumors (12). The violin plots represent the integrated RNASeq data from both TCGA and Genotype-Tissue Expression (GTEx), providing the comprehensive visualization of GLDC expression in OC tissues. One-way Analysis of Variance (ANOVA) p value was calculated across OC stages.

The progression-free survival (PFS) and overall survival (OS) analysis were performed using databases from the Kaplan-Meier Plotter (<http://kmplot.com/analysis>). Kmplot.com platform shows the

relationship between gene expression level and clinical outcomes of patients with OC (13). Patients with GLDC expression level above median value were arranged into the “high expression” group whereas those with GLDC expression level below median value were chosen into the “low expression” group. *p* value of < 0.05 was considered to indicate statistical significance.

2.2. Cell culture and reagents:

Human OC cell lines, including A2780, OVCAR3, and OVCAR8, were purchased from the Korean Cell Line Bank (KCLB, Seoul, Korea). CP-resistant OC cells, A2780-CP, were established by exposing A2780 cells to gradually increasing doses of CP, then continuously selecting colonies until 5 μ M CP resistance. OC cells were grown in culture media Roswell Park Memorial Institute 1640 (RPMI 1640, Invitrogen, Walham, MA, USA) supplemented with 10% fetal bovine serum (FBS, Welgene, Gyeonsangbuk-do, Korea), 1% antibiotic-antimycotic solution (Gibco, Grand Island, New York) in an incubation at 37 °C and 5% CO₂ humidified atmosphere.

CP (#15663-27-1) was purchased from Sigma-Aldrich (St. Louis, MO, USA). MitoTEMPO (MT, #HY-112879), Mdivi-1 (#HY-15886), and B106 (#HY-117800) were purchased from MedchemExpress (Seoul, Korea).

2.3. Transfection and stable cell line construction:

OC cells were plated in 60 mm dishes for 24 hr (2×10^5 cells per dish), then transfected with the desired plasmids and transfection reagents as follows: To perform knockdown of GLDC, the siRNA

targeting GLDC (#NM_000170.2, Bioneer, Daejeon, Korea) was transfected to A2780-CP cells with Oligofectamin Transfection reagent (#12252011, Invitrogen, Walham, MA, USA).

To establish stable OVCAR8 cells overexpressing GLDC, pcDNA3.1+-Flag-GLDC plasmid (#NM_000170.3, GenScript, Gyeonggi-do, Korea) was transfected into OVCAR8 cells using Lipofectamin 2000 (#11668019, Invitrogen, Walham, MA, USA).

2.4. Cell viability assay:

To examine the cytotoxic effect of various drugs in combination treatment with CP, the cell viability assay was performed using Cell Counting Kit-8 (CCK-8, Dogindo, Nagasaki, Japan). OC cells were plated in 96-well plates for 24 hr (3×10^3 cells per well), then treated with the drug concentrations adjusted following each experimental design. The treatment period lasts for 3 days, and the absorbance of formazan product was read at a wavelenth of 450 nm using TECAN Microplate Reader (TECAN, Mannedolf, Switzerland).

2.5. Fluorescence-activated cell sorting (FACs):

To measure mtROS level, OC cells were seeded in 6-well plates (5×10^5 cells per well) for 24 hr. Cells were collected by trypsinization (Invitrogen, Walham, MA, USA), then washed once using phosphate-buffered saline (PBS) buffer (Invitrogen, Walham, MA, USA). Cells were stained with mitoSOX (#M36008, Invitrogen, Walham, MA, USA) at working concentration of 5 μ M. Cells were incubated in a shaking incubator in 37 °C in 20 min. After that, cells were washed

twice using PBS buffer, then mtROS was detected using Phycoerythrin (PE) color laser. The relative mtROS level was analyzed using FACs Canto II flow cytometer (BD, Franklin, NJ, USA) and displayed using Flowjo software (Ashland, OR, USA).

2.6. Western blotting:

Harvested cell pellets were lysed using NP-40 buffer (1% NP-40, 40 mM Tris-HCl pH 8.0, 150 mM NaCl) containing protease inhibitor cocktails (PI) (Gendepot, Katy, TX, USA) and 0.2 M phenylmethylsulfonyl fluoride (PMSF) (Thermo Scientific, Boston, MA, USA), then centrifuged at 12,000 rpm in 30 min at 4 °C.

The protein concentration of the supernatant was quantified using BCA Protein Assay Kit (Thermo Scientific, Boston, MA, USA). Equal amounts of total proteins (30 µg) in each sample was prepared and separated by 8–15% sodium dodecyl sulphate polyacrylamide gel electrophoresis (SDS-PAGE), then transferred to nitrocellulose membranes 0.2 µm (Amersham Bioscience, Buckinghamshire, UK). The membranes were blocked in 5% bovine serum albumin (BSA) in Tris-buffered saline with Tween 20 (TBS-T) (50 mM NaCl, 10 mM Tris-HCl, 0.25% Tween-20) for 30 min at room temperature (RT), and then incubated with primary antibodies (Table 1) overnight at 4 °C. The membranes were incubated with the second antibodies (1:5,000 dilution, Santa Cruz Biotechnology, TX, USA) were applied to membranes for 2 hr at RT. The protein expression levels were detected using ChemiDoc™ MP Imaging System (Bio-Rad Laboratories, CA, USA).

2.7. *In vivo* xenograft model:

Female NOD/ShiLTJ-Rag2^{em1AMC}Ilrg^{em1AMC} (NRGA) mice at 6 wk of age were purchased from Ja Bio (Gyeonggi-do, Korea). According to the procedures from School of Medicine, Keimyung University (KM-2020-08R1), mice were randomly allocated to their cages (6 mice per group) in a standardized environmental condition for 2 wk. Human OC cells (1×10^7 cells per flank) were transplanted subcutaneously (s.c.) into the NRGA mice. When the tumor size reached 300 mm³, mice were intraperitoneally (i.p.) injected three times per wk for 2 wk with CP 3 mg/kg or saline. Tumor volume was measured three times per wk from the time of injection with a caliper in two dimensions. The volume (V) of individual tumor was calculated using the formula $V = 0.5 \times (\text{length (mm)} \times [\text{width (mm)}]^2)$.

2.8. Immunohistochemistry (IHC) analysis:

Mice-derived tumor tissues were fixed in 4% paraformaldehyd (PFA), and then formed into paraffin blocks. The fixed tissues were sliced into a thickness of 5 μ m sections using a Microtome (HM 325 Rotary Microtome, Thermo Scientific, Boston, MA, USA). The sections were dried at 60 °C in 30 min, then rehydrated through xylene, a graded series of ethanol, and 10% hydrogen peroxide (H₂O₂). For antigen retrieval, sections were filled in citrate medium (10 mM sodium citrate, 0.05% Tween 20, pH 6.0) at 95 °C. Sections were incubated with cleaved caspase-3 antibody (1:250 dilution, Cell Signalling Technology, MA, USA) and pDRP1 Ser616 (1:50 dilution, Cell Signalling Technology, MA, USA) at 4 °C overnight. The sections were incubated with secondary antibody (1:200 dilution, Santa Cruz Biotechnology, TX, USA) at 4 °C overnight. The positive signals were detected using

3,3'-diaminobenzidine (DAB) substrate kit (Vector Laboratories, Burlingame, CA, USA). Stained sections were visualized by DM750 microscopy (Leica, Wetzlar, Germany).

2.9. Immunofluorescence staining:

To measure Ki-67 staining, cells were plated in the coverslips in 24-well plates (1×10^4 cells per well) for 24 hr, and then treated with different doses of CP for 24 hr. Then, cancer cells on the coverslips were fixed in 4% PFA for at least 30 min at RT. Permeabilization was carried out using 0.1% Triton X-100 for 10 min, and non-specific binding was blocked using 1% BSA for 1 hr. Staining was performed by using the primary antibody Ki-67 (1:400 dilution, Abcam, Cambridge, UK) overnight at 4 °C. Samples were incubated with the secondary antibody (1:1,000 dilution, Santa Cruz Biotechnology, TX, USA) for 2 hr, then nucleus were stained by 1 μ g/mL 4',6-diamidino-2-phenylindole (DAPI). Samples were then mounted and kept dry for 24 hr. The Ki-67-positive cells were imaged using Carl Zeiss LSM5 EXCITER (Carl Zeiss, Oberkochen, Germany).

To measure mitochondrial dynamics, cancer cells were transfected with pDsRed2-Mito plasmid (#632421, Takara Bio, CA, USA). After selection by G418 (1,000 μ g/mL, Invitrogen, Walham, MA, USA), cell colonies were picked and grown. Cells were prepared following the above protocol and visualized using LSM5 EXCITER microscope (Carl Zeiss, Oberkochen, Germany). Quantitative analysis of mitochondrial dynamics was calculated using Mitochondrial Analyzer (ImageJ, Bethesda, MD, USA).

2.10. Real-time reverse transcription-polymerase chain reaction (RT-PCR) analysis:

Total RNA was extracted using Trizol reagent (Invitrogen, Walham, MA, USA). Extracted mRNA levels were quantified using the NanodropTM 2000 (NanoDrop Technologies, Wilmington, DE, USA). Then, equal amount of RNA (4 μ g) was prepared to synthesize complementary DNA (cDNA) with Moloney Murine Leukemia Virus (M-MLV) reverse transcriptase (Promega, Madison, WI, USA). Using Go Taq Flexi DNA Polymerase (Promega, Madison, WI, USA), PCR amplification was performed in an Swift MaxPro Thermal Cycler (SWT-MXP, Esco Lifesciences, Singapore). To perform RT-PCR, cDNA was performed with SYBR Green PCR Master Mix using the LightCycler 96 instrument (Roche, Basel, Switzerland) with specific primer (Macrogen, Seoul, Korea) for targeted gene (Table 2). All experiments were performed in triplicate. After the reaction, mRNA expression levels were calculated using the comparative Ct ($2^{-\Delta\Delta C_t}$) method and were normalized to the levels of the respective housekeeping gene, *GAPDH*. All results are presented as mean fold change \pm standard errors.

2.11 Statistical analysis:

Data were generated with at least three independent experiments that represented as means \pm standard deviation (SD) ($n \geq 3$). Data were analyzed by Student's *t*-test with $p < 0.05$ being considered as statistical significance.

Table 1: Antibodies Used for Western Blotting

No.	Antibodies	Company	Observed molecular weight (kDa)	Identifier
1	anti-GAPDH	GeneTex, CA, USA	37	#GTX627408
2	anti-cleaved caspase-3	Cell signalling Technology, MA, USA	15-17	#9664
3	anti-cleaved PARP	Cell signalling Technology, MA, USA	88	#5625
4	anti- β -actin	Santa Cruz Biotechnology, TX, USA	42	#sc-47778
5	anti-pPKC Thr505	Cell signalling Technology, MA, USA	78	#9374
6	anti-PKC δ	Cell signalling Technology, MA, USA	78	#2058
7	anti-DRP1	Santa Cruz Biotechnology, TX, USA	80	#sc-271583
8	anti-pDRP1 Ser616	Cell signalling Technology, MA, USA	80	#3455

Table 2. Primer Pair Sequences Used for RT-PCR

<i>Gene</i>	Primers	℃	bp
<i>GLDC</i>	Forward : 5' - CTGCTGTGCTACTGACCTTTT - 3'	60	175
	Reverse : 5' - CCAGGCATCATTCCTCACCAAG - 3'		
<i>GAPDH</i>	Forward : 5' - GGCCTCCAAGGAGTAAGACC - 3'	60	147
	Reverse : 5' - AGGGGTCTACATGGCAACTG - 3'		

3. Results

3.1. High expression level of GLDC is correlated with poor survival rates in patients with OC:

To comprehensively evaluate the expression of GLDC across the ten most common cancers in women worldwide, 56,938 samples were obtained from TCGA databases in TNMplot analysis. The pan-cancer heat map revealed a notably higher expression of GLDC in OC tissues than normal ovary tissues, but this pattern was not observed in other types of cancers (Figure 1A). Additionally, mRNA expression of GLDC was significantly upregulated in OC samples compared to normal tissues (Figure 1B). The mRNA expression of GLDC was found to increase according to the International Federation of Gynecology and Obstetrics (FIGO) stages of epithelial OC (EOC) (Figure 1C), suggesting a potential role of GLDC in OC.

Furthermore, Kaplan–Meire survival analysis demonstrated that patients with high GLDC expression exhibited significantly lower OS and PFS rates than those with low GLDC expression (Figure 2A&B). These findings highlighted the potential role of GLDC as a prognosis biomarker in OC, promoting OC progression. Further research is necessary to elucidate the molecular mechanism by which GLDC contributes to OC progression.

3.2. CP-resistant OC cells were successfully established in *in vitro* and *in vivo* models:

To establish CP resistance in OC cells, parental A2780 cells were exposed to gradually increasing concentrations of CP, starting from 1 μ M and escalating to 5 μ M (Figure 3). As shown in Figure 4A, CP showed significant inhibitory effect on A2780 cells compared with CP-resistant A2780 (A2780-CP) cells, with IC_{50} values of 1.51 and 26.7 μ M, respectively. Trypan blue assay demonstrated a significantly higher rate of cell death in A2780 cells than A2780-CP cells (Figure 4B). Additionally, western blot analysis revealed an increase in apoptotic markers, including cleaved poly(ADP-ribose) polymerase (cleaved PARP) and cleaved caspase-3 in A2780, following 72 hr of CP treatment (Figure 4C).

To further investigate the cytotoxic effect of CP in two sub-cell lines in an *in vivo* model, sensitive and resistant OC cells were s.c. injected into NRGa mice to establish tumor xenograft model (Figure 5). Once the tumor became visible and reached a measurable size, the mice were i.p. injected with CP at a dose of 3 mg/kg. Notably, sensitive OC group exhibited a greater reduction in average tumor weight and volume than resistant OC group (Figure 6A&B). To demonstrate the cytotoxic effect of CP on OC tumors, I examined molecular marker of tumor apoptosis, cleaved caspase-3. Consistent with my *in vitro* observation, the expression of cleaved caspase-3 was increased in CP-treated sensitive OC group (Figure 6C), suggesting that CP effectively induced programmed cell death in the sensitive OC, but not chemoresistant OC. These results demonstrated the obstacles of CP resistance in OC treatment in both *in vitro* and *in vivo* models.

3.3. GLDC promotes CP resistance in OC cells:

Interestingly, after a short-time exposure of CP treatment, GLDC protein expression was upregulated in a time- and dose-dependent manner in parental A2780 cells (Figure 7A&B). These findings highlighted that CP not only induced apoptosis at high CP concentration or after prolonged treatment but also triggered adaptive cellular responses, such as enhanced GLDC expression. As expected, GLDC protein level was upregulated in A2780-CP compared to sensitive counterpart (Figure 7C). The mRNA expression analysis using RT-PCR revealed that the mRNA expression of GLDC in A2780-CP was approximately three time higher than that in A2780 (Figure 7D).

To thoroughly certify the role of GLDC in CP-resistant OC, knockdown of GLDC was performed in CP-resistant cells to assess its impact on drug resistance (Figure 8A). As shown in Figure 8B, knockdown of GLDC in A2780-CP cells significantly decreased cell viability under CP treatment, overcoming chemoresistance in OC. Knockdown of GLDC reduced Ki-67 expression, a marker of cell proliferation, indicating that knockdown of GLDC restored CP sensitivity in OC through decreasing cell viability (Figure 8C). Furthermore, knockdown of GLDC in A2780-CP cells increased apoptotic cell population following CP treatment, as shown by increased sub-G1 phase detection using cell cycle (Figure 8D).

To investigate whether GLDC enhances chemoresistance in other OC cells, we compared GLDC protein levels across A2780, OVCAR3, OVCAR8, and A2780-CP cells (Figure 9A). The results showed that OVCAR3 cells exhibited a high expression of GLDC, whereas OVCAR8 cells displayed a low expression of GLDC. Knockdown of GLDC in

OVCAR3 coupled with the increased sensitivity to CP treatment (Figure 9B). Conversely, overexpression of GLDC in OVCAR8 enhanced cell resistance against CP treatment (Figure 9C). These results indicated that GLDC plays a significant role in supporting cancer cells in evading chemotherapy-induced apoptosis, thereby promoting chemoresistance in OC.

3.4. GLDC enhances mtROS generation in CP-resistant OC cells:

CP exerts its anti-cancer effects by causing DNA damage in cancer cells, leading to increased mtROS generation, subsequently contributing to cellular apoptosis (14,15). However, cancer cells might trigger other mechanisms to mitigate mtROS-induced damage, resulting CP resistance (16). To investigate the relationship between CP-resistant OC cells and mtROS, the mtROS levels were measured in A2780-CP and parental A2780 cells. The result showed that A2780-CP cells exhibited higher relative mtROS level than A2780 (Figure 10A). Knockdown GLDC in CP-resistant cells decreased mtROS level (Figure 10B). These results suggested that CP-resistant OC cells upregulated GLDC and activated mtROS level, which might contribute to adaptive responses in OC cells. Similarly, OVCAR8 overexpressing GLDC promoted significantly higher mtROS production (Figure 10C), while knockdown of GLDC in OVCAR3 reduced mtROS level (Figure 10D).

Furthermore, MitoTEMPO (MT), a mitochondrial-targeted antioxidant, at 20 μ M effectively inhibited mtROS level in A2780-CP cells (Figure 11A). The combined treatment of CP and MT showed a synergistic effect in overcoming chemoresistance in OC (Figure 11B). Collectively,

these findings underscored the therapeutic potential of targeting GLDC-mediated mtROS in overcoming CP resistance in OC.

3.5. GLDC promotes mitochondrial fission in CP-resistant OC cells:

Previous studies have shown that mitochondrial fission enables OC cells to adapt to chemotherapeutic stress by maintaining mitochondrial function (17). This process, which involves dividing mitochondria into smaller units, enhances energy regulation, and their ability to survive during chemotherapy (18). As shown in Figure 12A, mitochondrial fragmentations were significantly increased in A2780-CP cells. Knockdown GLDC in CP-resistant cells inhibited the mitochondrial fission (Figure 12B). Conversely, overexpression of GLDC in OVCAR8 increased mitochondrial fission, which in turn improved mitochondrial function and evaded cytotoxic stress of CP (Figure 12C). The protein DRP1 is central to the mitochondrial fission process, with phosphorylation of DRP1 at Serine 616 (pDRP1 Ser616) serving as a key marker of mitochondrial fission (19). As shown in Figure 12D&E, a significant increase in pDRP1 Ser616 was observed in A2780-CP cells in both *in vitro* and *in vivo* models. Knockdown of GLDC in A2780-CP cells notably reduced pDRP1 Ser616 (Figure 12F), indicating that GLDC upregulation promoted DRP1-induced mitochondrial fission in CP-resistant OC cells.

Additionally, the DRP1-induced mitochondrial fission inhibitor, Mdivi-1, reduced the mitochondrial fission by inhibiting the phosphorylation of

DRP1 at Serine 616 (20) (Figure 13A), and inhibited cell viability in a combination with CP (Figure 13B). Importantly, inhibition of mitochondrial fission did not affect mtROS level (Figure 13C), indicating that mtROS was an upstream of mitochondrial fission and activated the process of mitochondrial fission in response to CP-induced oxidative stress. In contrast, treatment with MT, mtROS inhibitor, decreased pDRP1 Ser616 level, further suggesting that mtROS regulated mitochondrial fission through the activation of DRP1 in CP-resistant OC cells (Figure 13D). These findings suggested that GLDC-driven mtROS acted as a regulatory signal for mitochondrial fission in CP-resistant OC cells.

3.6. GLDC promotes mitochondrial fission via mtROS-induced PKC δ phosphorylation in CP-resistant OC cells:

Protein kinase C delta (PKC δ) is a well-known serine/threonine kinase to regulate mitochondrial dynamics, particularly phosphorylating DRP1 at Serine 616, promoting mitochondrial fission (21). Phosphorylation of PKC δ at Threonine 505 (pPKC δ Thr505) activates enzyme activity and stability (22,23). As shown in Figure 14A, pPKC δ Thr505 was increased in A2780-CP cells. Knockdown of GLDC in A2780-CP significantly decreased both pPKC δ Thr505 and pDRP1 Ser616 (Figure 14B). Overexpression of GLDC in OVCAR8 led to the similar upregulation of pPKC δ Thr505 (Figure 14C), whereas knockdown of GLDC in OVCAR3 reduced the pPKC δ Thr505 (Figure 14D). These results indicated that GLDC induced pPKC δ Thr505, ultimately contributing to CP resistance in OC cells.

In CP-resistant OC cells, treatment of MT significantly decreased

protein expressions of both pPKC δ Thr505 and pDRP1 Ser616 (Figure 15A), suggesting that mtROS acted as an upstream of PKC δ activation. However, Mdivi-1 did not change the pPKC δ Thr505 (Figure 15B), which supported the hypothesis that mtROS-driven PKC δ activation led to DRP1-dependent mitochondrial fission in CP-resistant OC cells. Moreover, B106, which induced the reduction of pPKC δ Thr505 protein expression (Figure 15C), significantly decreased cell viability in A2780-CP (Figure 15D), further emphasizing the biological role of PKC δ activation in supporting OC cell survival under CP-induced stress environment. Taken together, these results implied that the GLDC-driven mtROS generation stimulated the phosphorylation of PKC δ , leading to DRP1-dependent mitochondrial fission in CP-resistant OC cells (Figure 16).

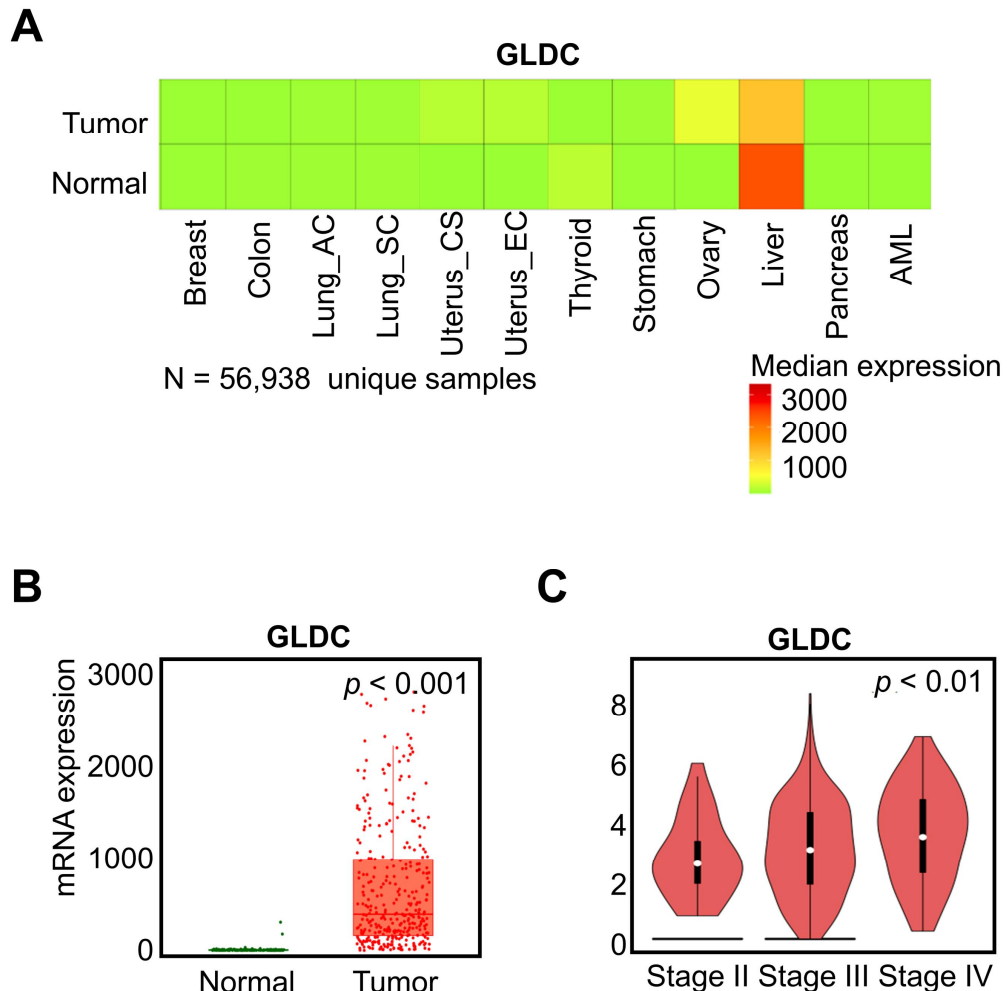


Figure 1. Analysis of GLDC gene expression in cancers. (A) Pan-cancer heatmap compared the gene expression of GLDC in various cancer types using TCGA database. (B) GLDC mRNA expression was analyzed in tumor tissues compared with normal tissues in ovarian cancer using TNMplot (<https://tnmplot.com/analysis>). (C) The gene expression of GLDC was analyzed according to ovarian cancer stages using GEIPA web server (<http://gepia.cancer-pku.cn/index.html>). GLDC: Glycine

decarboxylase, Lung_AC: Lung adenocarcinoma, Lung_SC:
Lung small cell carcinoma, Uterus_CS: Uterus
carcinosarcoma, Uterus_EC: Uterus endometrial carcinoma,
AML: Acute myeloid leukemia.

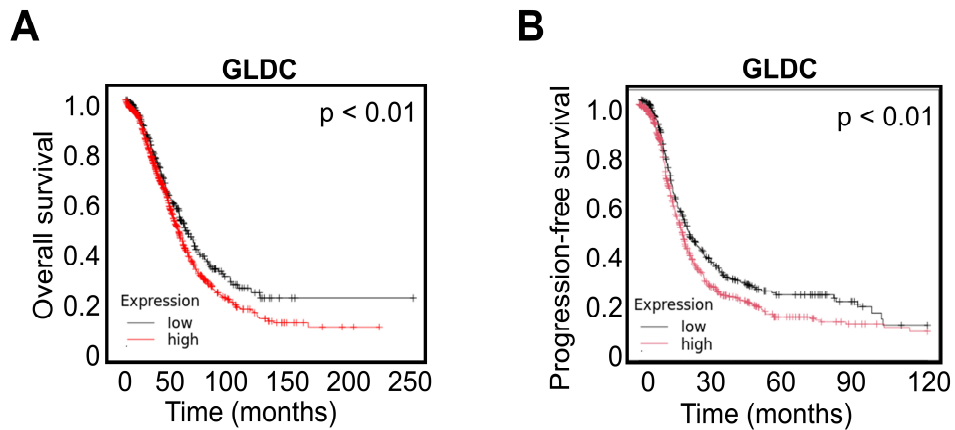


Figure 2. Survival analysis of GLDC in patients with ovarian cancer.

Kaplan-Meire analysis of (A) 20-yr overall survival and (B) 10-yr progression-free survival were compared between high and low GLDC expression groups (<https://kmplot.com/analysis>). GLDC: Glycine decarboxylase.

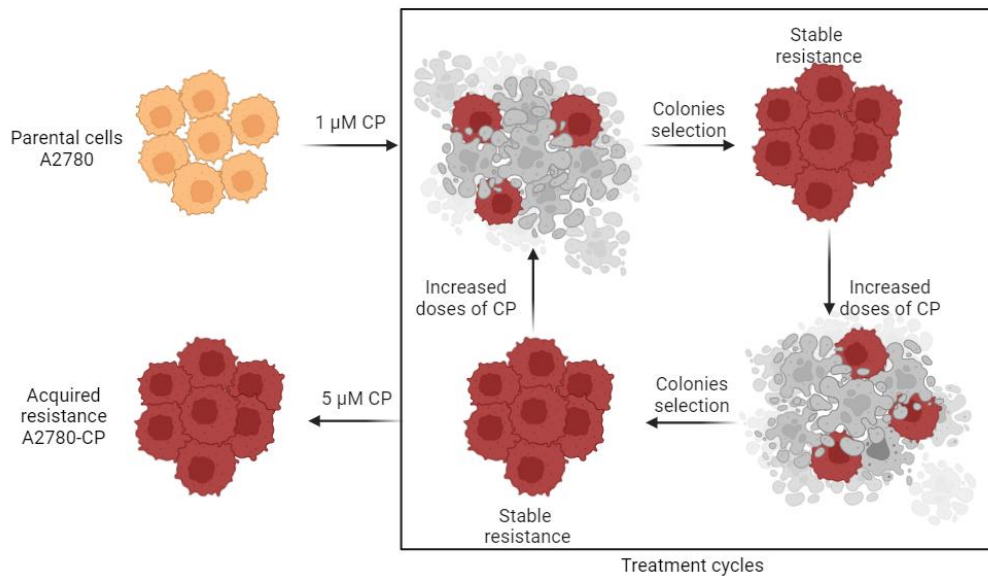


Figure 3. Scheme of establishment of CP-resistant ovarian cancer cells in an *in vitro* model. CP-resistant ovarian cancer cells (A2780-CP) were developed by long-term exposure to gradually increasing concentrations of CP (<https://app.biorender.com>). CP: Cisplatin.

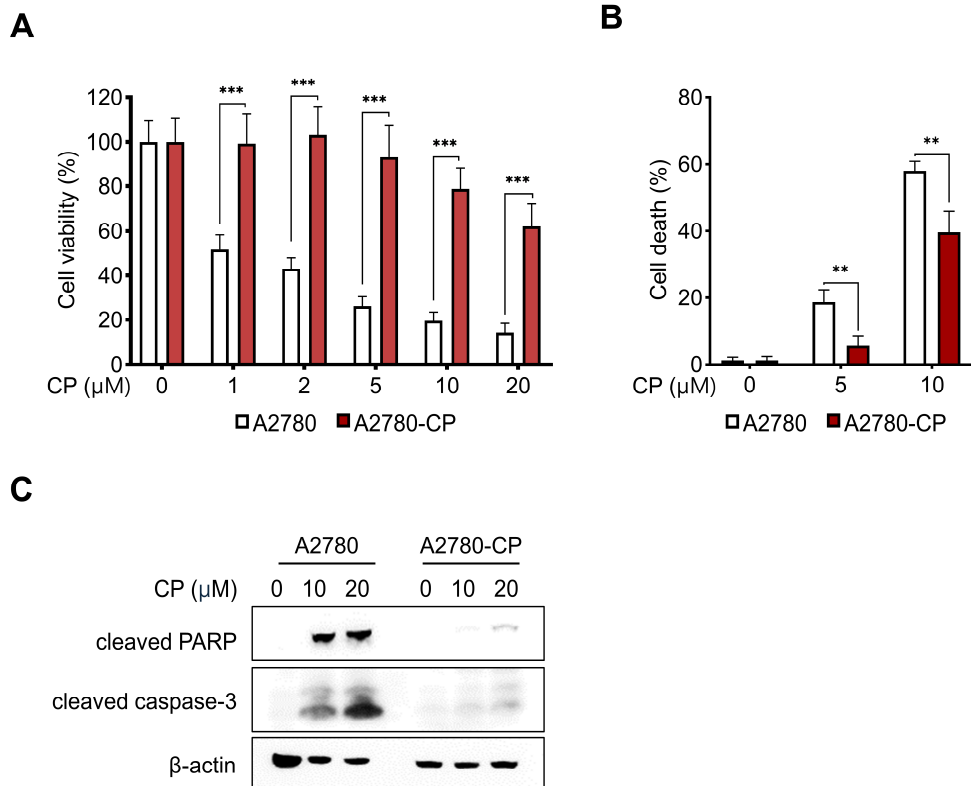


Figure 4. Cytotoxic effect of CP on resistant and parental ovarian cancer cells in an *in vitro* model. (A) The inhibitory effect of CP was examined on A2780 compared with A2780-CP. Cells were treated with CP at the indicated doses for 3 days. Cell viability was measured using CCK-8 assay. (B) The number of cell death was measured in A2780 compared with A2780-CP using trypan blue assay. Cells were treated with CP at the indicated doses for 3 days. (C) Apoptotic markers were detected using western blotting. All data are presented as the mean \pm SD (n = 5). Significant differences are indicated: ***: $p < 0.001$, **: $p < 0.01$. CP: Cisplatin, Cleaved PARP: Cleaved poly(ADP-ribose) polymerase, CCK8: Cell Counting Kit-8.

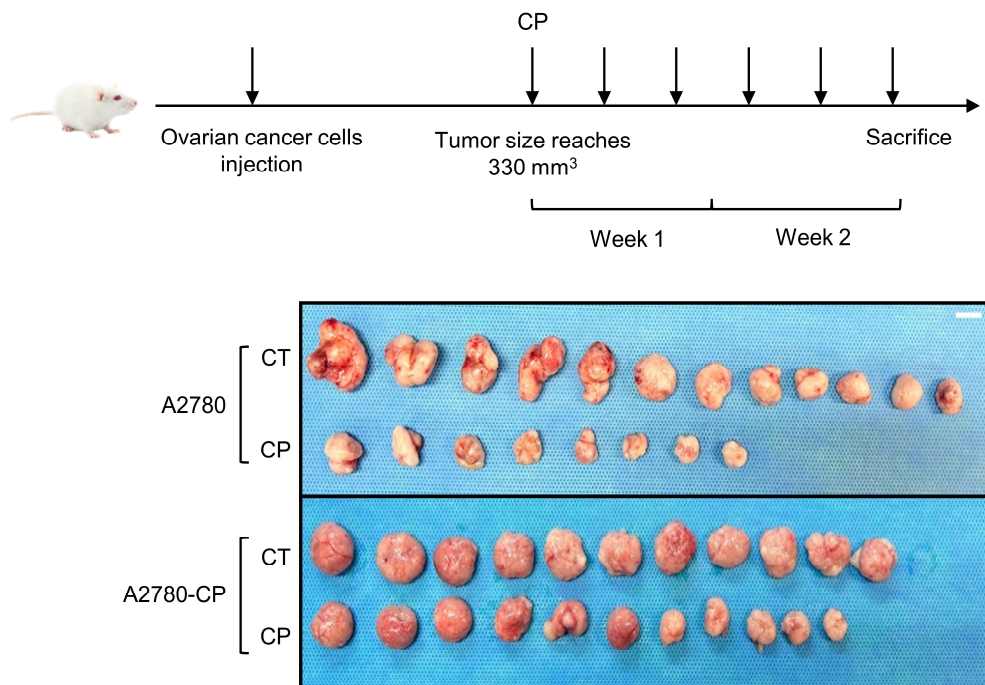


Figure 5. Scheme of an *in vivo* experiment to examine the cytotoxic effect of CP on ovarian cancer. Schematic drawing described the experimental plan for the *in vivo* study performed in a mouse model in the upper panel. After CP administration, the tumors were collected and displayed in the lower panel. CT: Control, CP: Cisplatin. Bar, 10 mm.

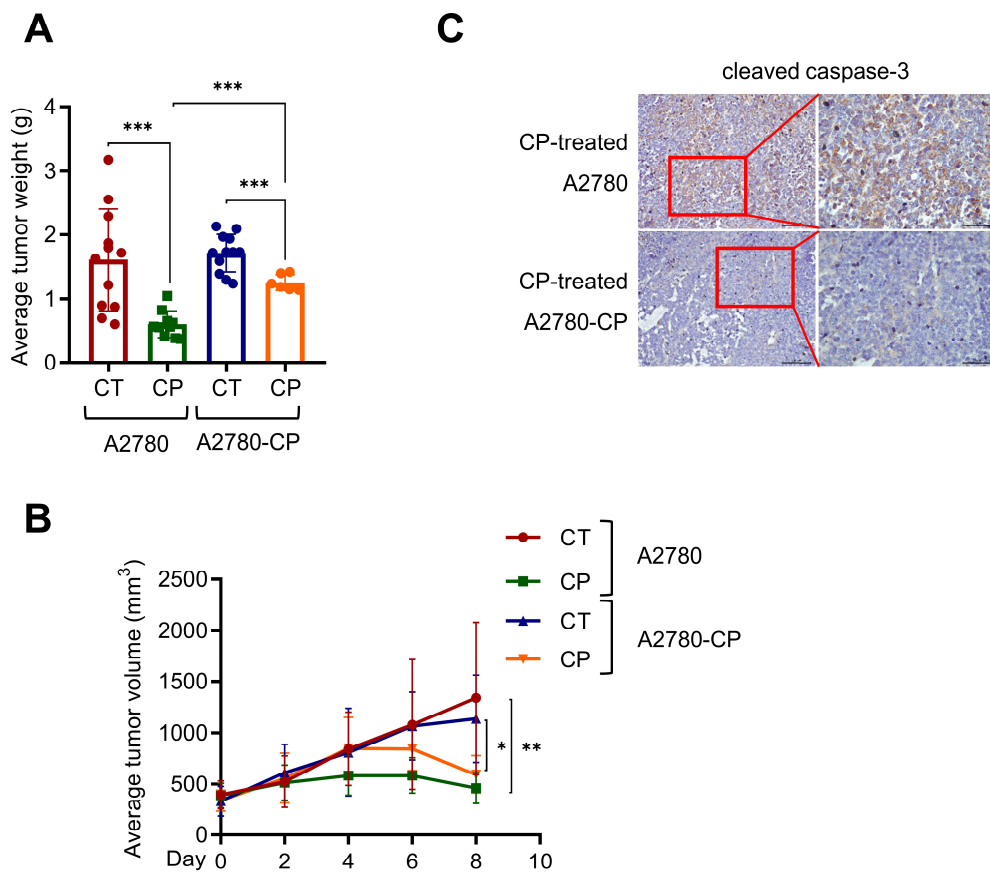


Figure 6. Cytotoxic effect of CP on ovarian cancer cells in an *in vivo* model. Average tumor weight (**A**) and average tumor volume (**B**) were analyzed in A2780-injected mice compared with A2780-CP-injected mice. (**C**) Cleaved caspase-3, an apoptotic marker, were detected using IHC staining. All data are presented as the mean \pm SD (n = 12). Significant differences are indicated: ***: $p < 0.001$, **: $p < 0.01$, *: $p < 0.05$. CT: Control, CP: Cisplatin, IHC: Immunohistochemistry.

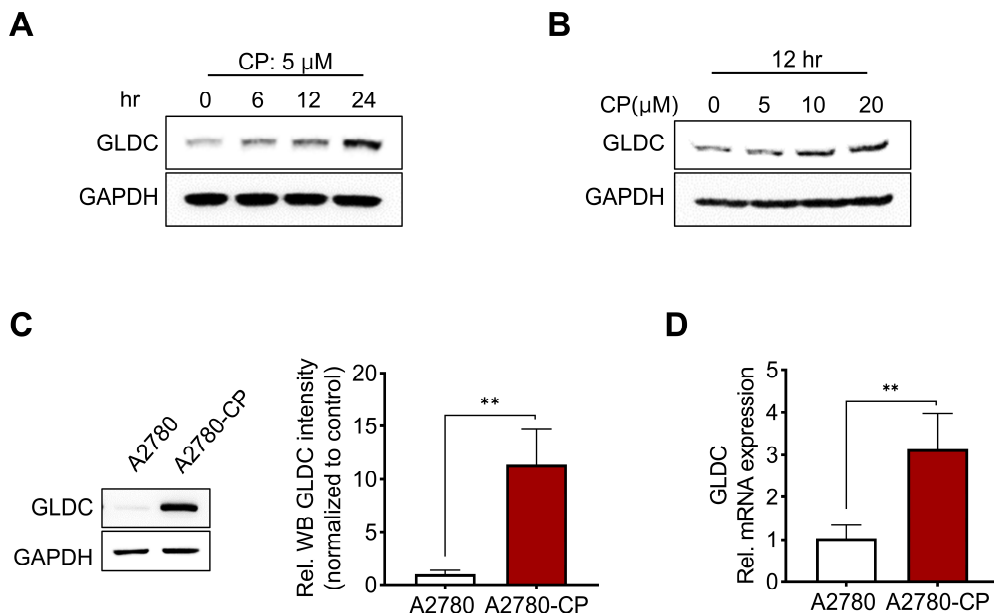


Figure 7. Analysis of GLDC expression in CP-resistant ovarian cancer cells. GLDC protein expression was detected in parental A2780 cells following (A) a time- and (B) dose-dependent manner. (C) GLDC protein level was detected in comparison of A2780 and A2780-CP cells using western blotting in the left panel. Quantification of western blotting bands were shown in the right panel. (D) The mRNA expression of GLDC was detected in comparison between A2780-CP and A2780 cells. All data are presented as the mean \pm SD (n = 3). Significant difference is indicated: **: $p < 0.01$. GLDC: Glycine decarboxylase, GAPDH: Glyceraldehyde 3-phosphate dehydrogenase, CP: Cisplatin, Rel: Relative.

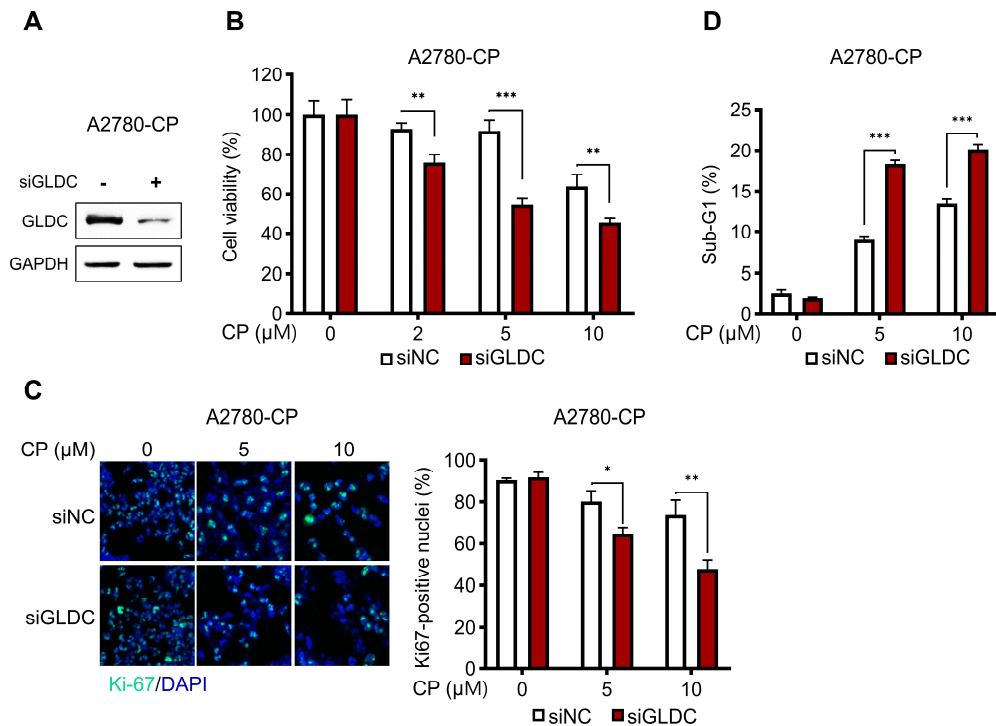


Figure 8. Analysis of knockdown GLDC in CP-resistant ovarian cancer cells. (A) Knockdown of GLDC was carried out in CP-resistant cells. (B) Cell viability was measured after knockdown GLDC in A2780-CP cells. Cells were treated with CP at the indicated doses for 3 days. (C) Ki-67 expression was detected using immunofluorescence staining. Cells were treated with CP at the indicated doses for 24 hr. (D) Apoptotic cell population was calculated by sub-G1 phase detection using FACs. All data are presented as the mean \pm SD ($n = 3$). Significant differences are indicated: ***: $p < 0.001$, **: $p < 0.01$, *: $p < 0.05$. GLDC: Glycine decarboxylase, GAPDH: Glyceraldehyde 3-phosphate dehydrogenase, CP: Cisplatin, siNC: siRNA negative control, DAPI: 4',6-diamidino-2-phenylindole.

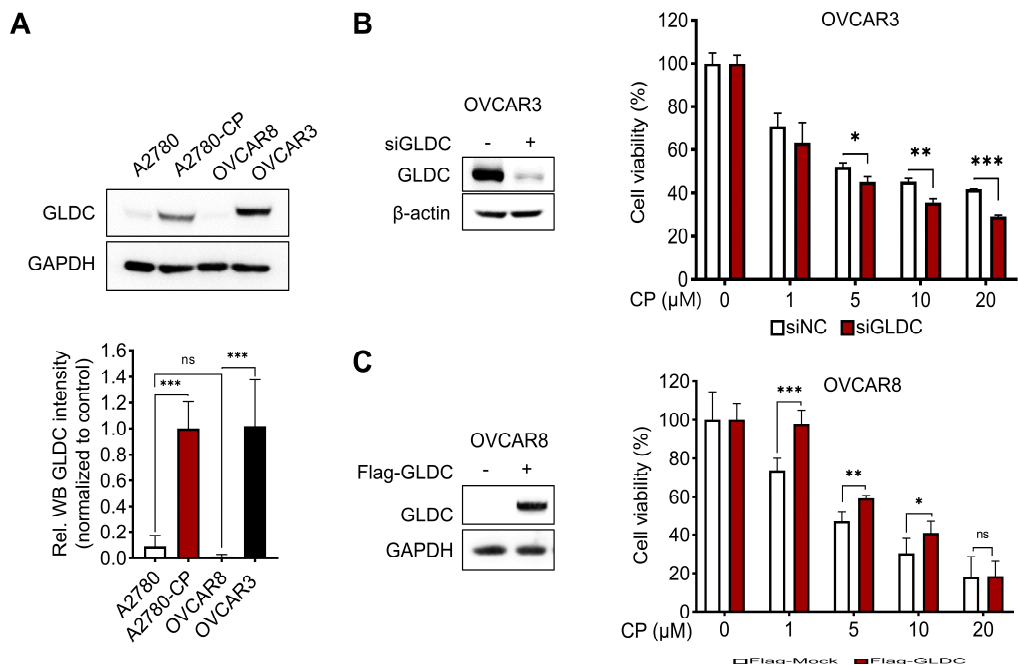


Figure 9. Analysis of GLDC function in CP resistance across various types of ovarian cancer cells. (A) GLDC protein levels were examined across A2780, OVCAR3, OVCAR8, and A2780-CP cells in the upper panel. Quantification of protein levels were shown in the lower panel. (B) Knockdown GLDC was performed in OVCAR3 cells in the left panel. Cell viability of OVCAR3 was shown in the right panel. (C) Overexpression of GLDC was performed in OVCAR8 in the left panel. Cell viability of OVCAR8 was shown in the right panel. All ovarian cancer cells were treated with CP at the indicated doses for 3 days. All data are presented as the mean \pm SD ($n = 3$). Significant differences are indicated: ***: $p < 0.001$, **: $p < 0.01$, *: $p < 0.05$, ns: non significance. CP: Cisplatin, Rel: Relative, GLDC: Glycine decarboxylase, GAPDH: Glyceraldehyde 3-phosphate dehydrogenase, siNC: siRNA negative control.

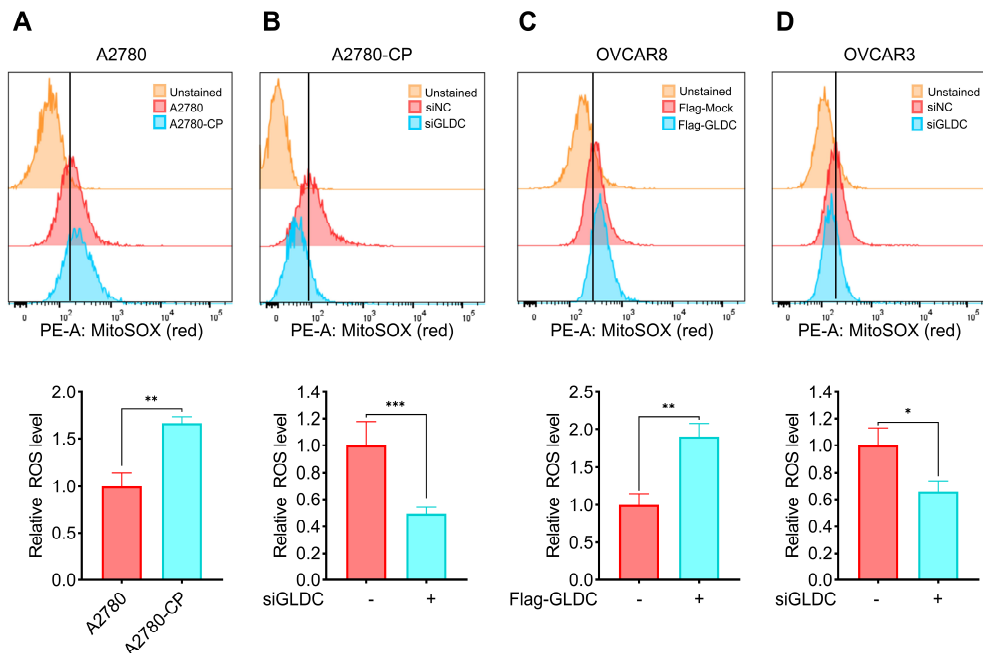


Figure 10. Analysis of relative mtROS level in ovarian cancer cells.

(A) mtROS was examined in comparison of parental A2780 and A2780-CP in the upper panel. The graph result was represented in the bottom panel. (B) mtROS level was measure after knockdown of GLDC in A2780-CP cells in the upper panel. The bottom panel presented the statistical result. (C) mtROS level was detected in comparison between overexpression of GLDC in OVCAR8 with controls in the upper panel. The bottom panel represented the statistical result. (D) mtROS level was detected in comparison between knockdown of GLDC in OVCAR3 with controls in the upper panel. The bottom panel represented the statistical result. All data are presented as the mean \pm SD (n = 3). Significant differences are indicated: ***: $p < 0.001$, **: $p < 0.01$, *: $p < 0.05$. CP: Cisplatin, GLDC: Glycine decarboxylase, siNC: siRNA negative control.

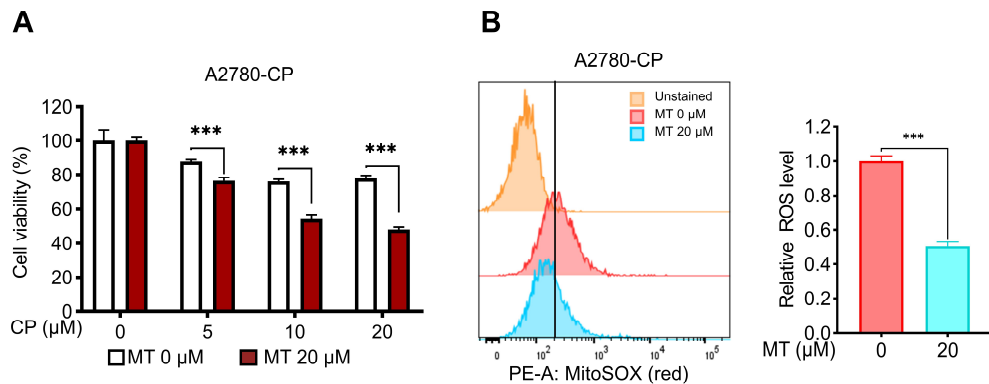


Figure 11. Synergistic effect of MT on CP-resistant ovarian cancer cells. (A) The combined treatment of CP and MT was examined in CP-resistant ovarian cancer cells. Cells were treated with CP and MT at the indicated doses for 3 days. Cell viability was measured using CCK-8 assay. (B) mtROS level was measured after exposing to MT in A2780-CP cells in the left panel. The graph result was represented in the right panel. All data are presented as the mean \pm SD ($n = 3$). Significant difference is indicated: ***: $p < 0.001$. CP: Cisplatin, MT: MitoTEMPO, CCK8: Cell Counting Kit-8.

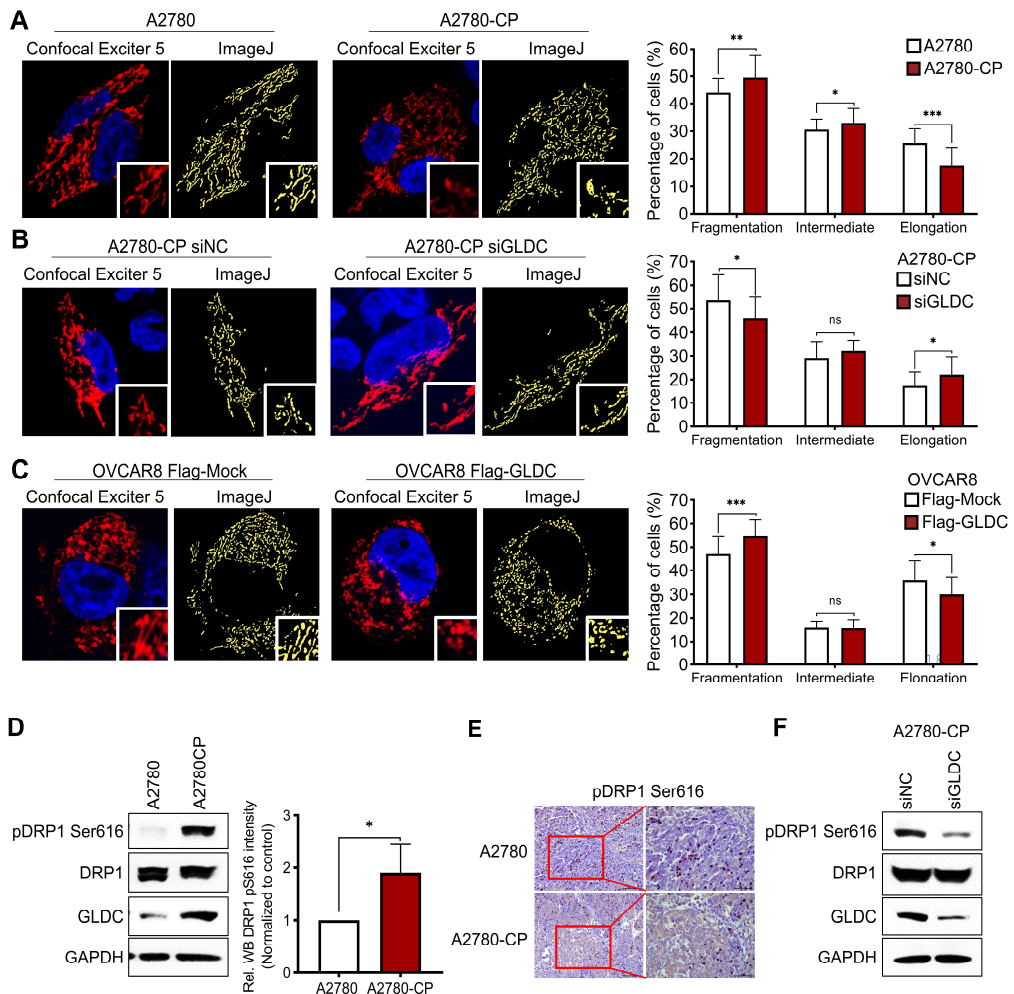


Figure 12. Analysis of mitochondrial fission in CP-resistant ovarian cancer cells. (A) Mitochondrial fragmentation was analyzed in comparison of A2780 and A2780-CP cells in the left panel. The graph result was represented in the right panel. (B) Mitochondrial fission was analyzed after knockdown of GLDC in CP-resistant cells in the left panel. The graph result was represented in the right panel. (C) Mitochondrial fission was examined in OVCAR8 overexpressing GLDC in

the left panel. The graph result was represented in the right panel. **(D)** pDRP1 Ser616 expression was detected in comparison between A2780 and A2780-CP in the left panel. The graph result was represented in the right panel. **(E)** pDRP1 Ser616 signal was detected in A2780-CP-injected tumors in an *in vivo* model using IHC staining. **(F)** pDRP1 Ser616 was detected after knockdown of GLDC in A2780-CP cells. All data are presented as the mean \pm SD (n = 3). Significant differences are indicated: ***: $p < 0.001$, **: $p < 0.01$, *: $p < 0.05$, ns: non significance. CP: Cisplatin, Rel: Relative, GLDC: Glycine decarboxylase, DRP1: Dynamin-related protein 1; pDRP1: Phosphorylation DRP1, GAPDH: Glyceraldehyde 3-phosphate dehydrogenase, IHC: Immunohistochemistry, siNC: siRNA negative control.

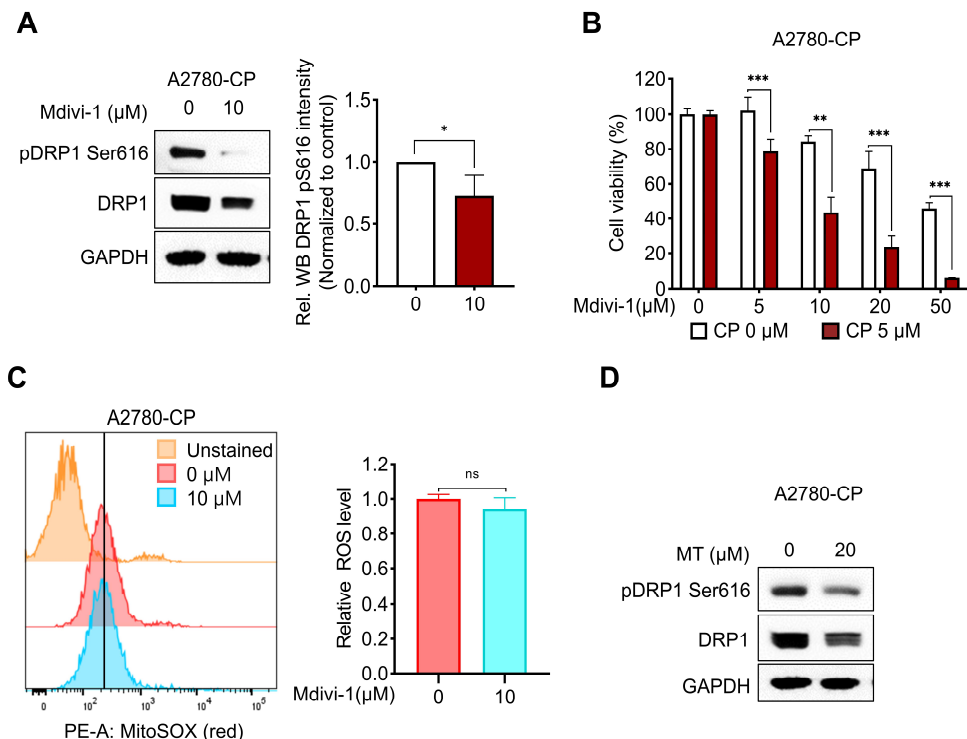


Figure 13. Analysis of mtROS-induced mitochondrial fission using Mdivi-1 treatment in CP-resistant ovarian cancer cells. (A) The protein level of pDRP1 Ser616 was detected after treatment with Mdivi-1. The western blotting bands were represented in the left panel. The graph result was represented in the right panel. (B) Cell viability was measured in the combination of Mdivi-1 with CP. Cells were treated with CP and Mdivi-1 at the indicated doses for 3 days. Cell viability was measured using CCK-8 assay. (C) mtROS level was measured after treatment with Mdivi-1 in the left panel. The graph result was represented in the right panel. (D) The protein level of pDRP1 Ser616 was detected after treatment with MT using western blotting. All data are presented as the mean \pm SD (n = 3).

Significant differences are indicated: ***: $p < 0.001$, **: $p < 0.01$, *: $p < 0.05$, ns: non significance. CP: Cisplatin, MT: MitoTEMPO, PKC δ : Protein kinase C δ , pPKC δ : Phosphorylation PKC δ , DRP1: Dynamin-related protein 1, pDRP1: Phosphorylation DRP1, GAPDH: Glyceraldehyde 3-phosphate dehydrogenase.

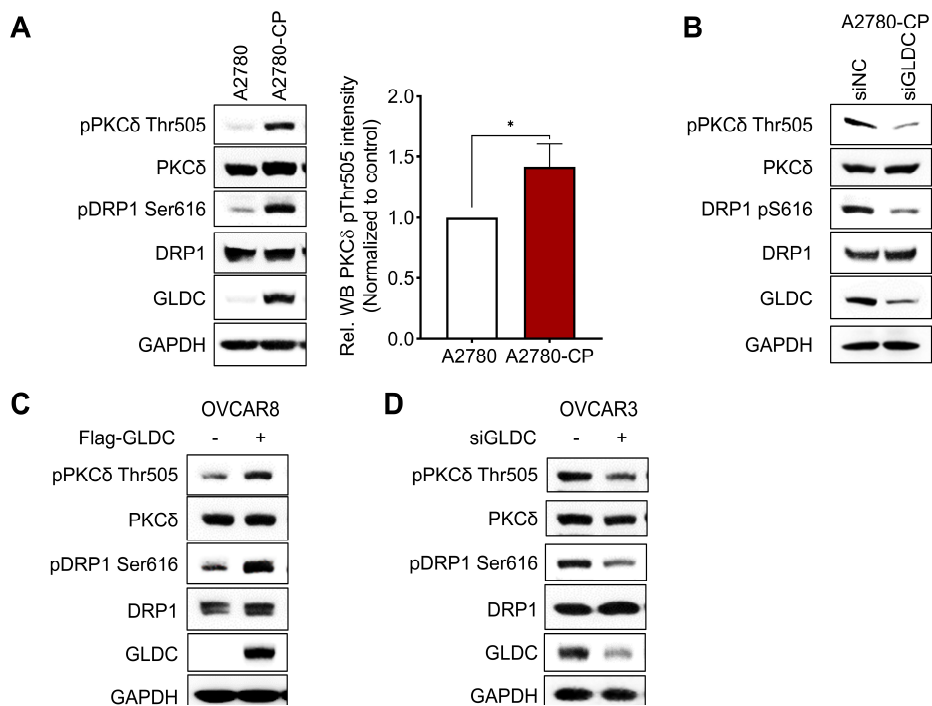


Figure 14. Analysis of PKCδ-induced mitochondrial fission in ovarian cancer cells. (A) pPKCδ Thr505 expression was detected in comparison between A2780-CP and A2780 cells in the left panel. The graph result was represented in the right panel. (B) pPKCδ Thr505 and pDRP1 Ser616 in A2780-CP was detected after knockdown of GLDC. (C) pPKCδ Thr505 was detected in OVCAR8 overexpressing GLDC. (D) pPKC Thr505 level was detected in GLDC knockdwon OVCAR3. All data are presented as the mean \pm SD (n = 3). Significant difference is indicated: *: $p < 0.05$. CP: Cisplatin, GLDC: Glycine decarboxylase, PKCδ: Protein kinase C δ , pPKCδ: Phosphorylation PKCδ, DRP1: Dynamin-related protein 1, pDRP1: Phosphorylation DRP1, GAPDH: Glyceraldehyde 3-phosphate dehydrogenase, Rel: Relative, siNC: siRNA negative control.

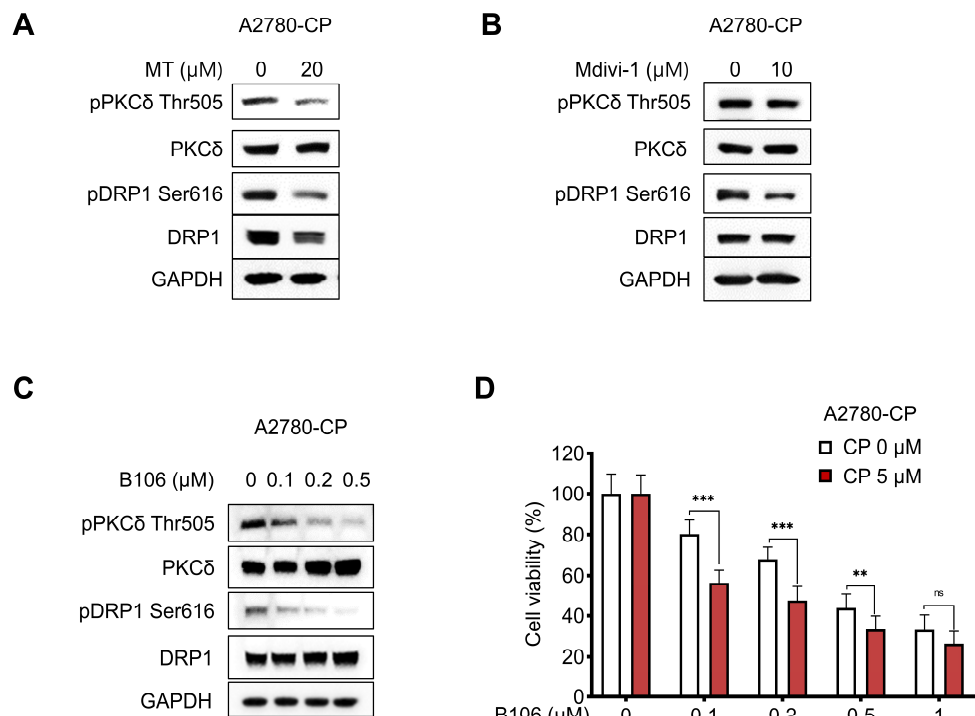


Figure 15. Analysis of mtROS-driven PKCδ phosphorylation using B106 treatment in CP-resistant ovarian cancer cells. (A) The protein expression levels of pPKCδ Thr505 and pDRP1 Ser616 were detected in A2780-CP after MT treatment. (B) The protein expression levels of pPKCδ Thr505 and pDRP1 Ser616 were detected in A2780-CP after Mdivi-1 treatment. (C) The protein expression levels of pPKCδ Thr505 and pDRP1 Ser616 were detected in A2780-CP after B106 treatment. (D) Cell viability was examined in A2780-CP in the combination treatment of B106 with CP. All data are presented as the mean ± SD (n = 5). Significant differences are indicated: ***: $p < 0.001$, **: $p < 0.01$, ns: non significance. CP: Cisplatin, MT: MitoTEMPO, PKCδ: Protein kinase C δ, pPKCδ: Phosphorylation PKCδ, DRP1: Dynamin-related protein 1, pDRP1: Phosphorylation DRP1.

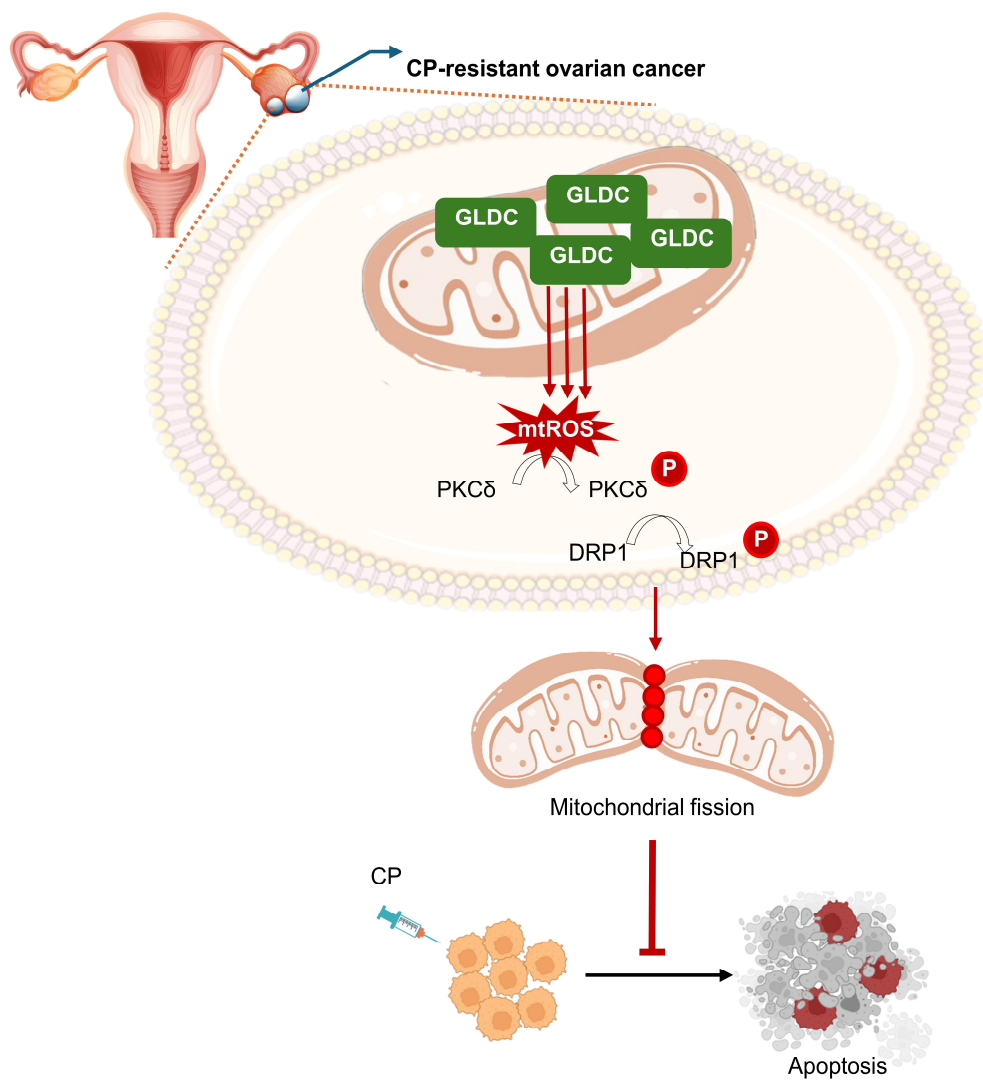


Figure 16. Schematic illustration of the main results of this study.

GLDC promotes CP resistance of ovarian cancer cells by enhancing mtROS-driven mitochondrial fission. (<https://app.biorender.com>). GLDC: Glycine decarboxylase, CP: Cisplatin, mtROS: Mitochondrial reactive oxygen species, PKCδ: Protein kinase C δ, DRP1: Dynamin-related protein 1.

4. Discussion

This study shows the potential oncogenic function of GLDC in promoting CP resistance in OC by demonstrating that GLDC enhances mtROS production, which subsequently activates pPKC δ Thr505, leading to DRP1-induced mitochondrial fission in CP-resistant OC cells.

GLDC is the hallmark regulator in glycine metabolic pathway. Previous studies demonstrated that in gastric (24) and HCC (25,26), GLDC acts as a tumor suppressor. However, GLDC acts as an oncogene in NSCLC (8) and neuroblastoma (9), promoting tumor progression and cell-initiating properties, which are consistent with my study. Therefore, therapeutic strategies targeting GLDC must be carefully considered depending on the specific cancer types.

The evidence suggests that oxidative stress is a key player in chemoresistant ovarian cancer. Figure 10&11 demonstrate that GLDC significantly enhances mtROS level in CP-resistant OC cells. However, the underlying molecular mechanism by which GLDC enhances mtROS production remains unclear. Previous study demonstrated that downregulation of GLDC raised cellular ROS levels through reducing GSH/GSSG ratio in HCC cells (25). Therefore, further studies are needed to determine the molecular mechanism underlying GLDC-induced mtROS in CP-resistant OC.

In this study, fragmented mitochondria facilitates CP resistance through mtROS in OC cells (Figure 12&13). The results of this study are consistent with recent research. Previous studies demonstrated that resistant OC cells present a more fragmented mitochondria than the sensitive counterparts (27-29). These findings highlight mitochondrial dynamic is a viable therapeutic target to mitigate chemoresistance.

As shown in Figure 15, B106 significantly decreased pPKC δ Thr505, resulting in cell sensitivity to CP treatment in OC. However, the effect of B106 on pPKC δ Thr505 is controversial (30). Therefore, the effect of B106 on pPKC δ Thr505 needs further investigation.

In conclusion, Figure 16 demonstrates that GLDC acts as an oncogene, promoting CP resistance in OC. GLDC increases PKC δ activation-induced mitochondrial fission by enhancing mtROS generation. This provides new evidence that GLDC-induced mtROS promotes CP resistance in OC cells and suggests that GLDC is a promising therapeutic target in chemoresistant OC treatment.

5. Summary

This study highlights the pivotal role of GLDC in promoting CP resistance in OC. Elevated expression of GLDC closely correlated with poor clinical outcomes in patients with OC. In an *in vitro* model, GLDC protein level in CP-resistant OC cells was significantly upregulated, whereas knockdown of GLDC restored their sensitivity to CP treatment, underscoring the critical role of GLDC in driving chemoresistance. Moreover, this study identified mtROS as the key downstream effector of GLDC-induced chemoresistance in OC. CP-resistant cancer cells exhibited both high GLDC expression and elevated mtROS level. Importantly, knockdown of GLDC reduced mtROS level, demonstrating that GLDC directly regulates mtROS to activate pro-survival pathways. Subsequently, elevated mtROS level activates pPKC δ Thr505, leading to DRP1-induced mitochondrial fission, a well-known process contributing to CP resistance in OC. Collectively, these findings indicated GLDC as a key regulator of CP resistance in OC, suggesting a potential therapeutic target in OC treatment.

References

1. Bray F, Ferlay J, Soerjomataram I, Siegel RL, Torre LA, Jemal A: Global Cancer Statistics 2018: GLOBOCAN Estimates of Incidence and Mortality Worldwide for 36 Cancers in 185 Countries. *CA Cancer J Clin* 2018; 68(6): 394-424.
2. Lheureux S, Braunstein M, Oza AM: Epithelial Ovarian Cancer: Evolution of Management in the Era of Precision Medicine. *CA Cancer J Clin* 2019; 69(4): 280-304.
3. Wright JD, Chen L, Tergas AI, Patankar S, Burke WM, Hou JY, et al.: Trends in Relative Survival for Ovarian Cancer from 1975 to 2011. *Obstet Gynecol* 2015; 125(6): 1345-52.
4. Lee JY, Kim S, Kim YT, Lim MC, Lee B, Jung KW, et al.: Changes in Ovarian Cancer Survival During the 20 Years before the Era of Targeted Therapy. *BMC Cancer* 2018; 18(1): 601-8.
5. Lheureux S, Gourley C, Vergote I, Oza AM: Epithelial Ovarian Cancer. *The Lancet* 2019; 393(10177): 1240-53.
6. Pignata S, C Cecere S, Du Bois A, Harter P, Heitz F: Treatment of Recurrent Ovarian Cancer. *Ann Oncol* 2017; 28(8): 51-6.
7. Go MK, Zhang WC, Lim B, Yew WS: Glycine Decarboxylase Is an Unusual Amino Acid Decarboxylase Involved in Tumorigenesis. *Biochem* 2014; 53(5): 947-56.

8. Zhang Wen C, Shyh-Chang N, Yang H, Rai A, Umashankar S, Ma S, et al.: Glycine Decarboxylase Activity Drives Non-Small Cell Lung Cancer Tumor-Initiating Cells and Tumorigenesis. *Cell* 2012; 148(1): 259-72.

9. Alptekin A, Ye B, Yu Y, Poole CJ, Van Riggelen J, Zha Y, et al.: Glycine Decarboxylase Is a Transcriptional Target of MYCN Required for Neuroblastoma Cell Proliferation and Tumorigenicity. *Oncogene* 2019; 38(50): 7504-20.

10. Mukha D, Fokra M, Feldman A, Sarvin B, Sarvin N, Nevo-Dinur K, et al.: Glycine Decarboxylase Maintains Mitochondrial Protein Lipoylation to Support Tumor Growth. *Cell Metab* 2022; 34(5): 775-82.

11. Bartha Á, Gyórfy B: TNMplot.com: A Web Tool for the Comparison of Gene Expression in Normal, Tumor and Metastatic Tissues. *Int J Mol Sci* 2021; 22(5): 2622-33.

12. Tang Z, Li C, Kang B, Gao G, Li C, Zhang Z: GEPIA: A Web Server for Cancer and Normal Gene Expression Profiling and Interactive Analyses. *Nucleic Acids Res* 2017; 45(1): 98-102.

13. Lánckzy A, Gyórfy B: Web-Based Survival Analysis Tool Tailored for Medical Research (KMplot): Development and Implementation. *J Med Internet Res* 2021; 23(7): 27633-9.

14. Mirzaei S, Hushmandi K, Zabolian A, Saleki H, Torabi SMR, Ranjbar A, et al.: Elucidating Role of Reactive Oxygen Species in

- Cisplatin Chemotherapy: A Focus on Molecular Pathways and Possible Therapeutic Strategies. *Molecules* 2021; 26(8): 2382–418.
15. Kleih M, Böpple K, Dong M, Gaißler A, Heine S, Olayioye MA, et al.: Direct Impact of Cisplatin on Mitochondria Induces ROS Production that Dictates Cell Fate of Ovarian Cancer Cells. *Cell Death Dis* 2019; 10(11): 851–62.
 16. Arfin S, Jha NK, Jha SK, Kesari KK, Ruokolainen J, Roychoudhury S, et al.: Oxidative Stress in Cancer Cell Metabolism. *Antioxidants* 2021; 10(5): 642–69.
 17. Chen W, Zhao H, Li Y: Mitochondrial Dynamics in Health and Disease: Mechanisms and Potential Targets. *Signal Transduct Target Ther* 2023; 8(1): 333–57.
 18. Ježek J, Cooper KF, Strich R: The Impact of Mitochondrial Fission–Stimulated ROS Production on Pro–Apoptotic Chemotherapy. *Biology* 2021; 10(1): 33–52.
 19. Chang CR, Blackstone C: Dynamic Regulation of Mitochondrial Fission through Modification of the Dynamin–Related Protein Drp1. *Ann NY Acad Sci* 2010; 1201(1): 34–9.
 20. Duan C, Wang L, Zhang J, Xiang X, Wu Y, Zhang Z, et al.: Mdivi-1 Attenuates Oxidative Stress and Exerts Vascular Protection in Ischemic/Hypoxic Injury by a Mechanism Independent of Drp1 GTPase Activity. *Redox Biol* 2020; 37(101706): 1016–29.

21. Lin AJ, Joshi AU, Mukherjee R, Tompkins CA, Vijayan V, Mochly-Rosen D, et al.: PKC δ -Mediated DRP1 Phosphorylation Impacts Macrophage Mitochondrial Function and Inflammatory Response to Endotoxin. *Shock* 2022; 57(3): 435-43.
22. Rybin VO, Guo J, Harleton E, Feinmark SJ, Steinberg SF: Regulatory Autophosphorylation Sites on Protein Kinase C-Delta at Threonine-141 and Threonine-295. *Biochem* 2009; 48(21): 4642-51.
23. Yang Q, Langston JC, Tang Y, Kiani MF, Kilpatrick LE: The Role of Tyrosine Phosphorylation of Protein Kinase C Delta in Infection and Inflammation. *Int J Mol Sci* 2019; 20(6): 1498-514.
24. Min HL, Kim J, Kim WH, Jang BG, Kim MA: Epigenetic Silencing of the Putative Tumor Suppressor Gene GLDC (Glycine Dehydrogenase) in Gastric Carcinoma. *Anticancer Res* 2016; 36(1): 179-87.
25. Zhuang H, Wu F, Wei W, Dang Y, Yang B, Ma X, et al.: Glycine Decarboxylase Induces Autophagy and is Downregulated by miRNA-30d-5p in Hepatocellular Carcinoma. *Cell Death Dis* 2019; 10(3): 192-205.
26. Zhuang H, Li Q, Zhang X, Ma X, Wang Z, Liu Y, et al.: Downregulation of Glycine Decarboxylase Enhanced Cofilin-Mediated Migration in Hepatocellular Carcinoma Cells. *Free Radic Biol Med* 2018; 120(3): 1-12.
27. Catanzaro D, Gaude E, Orso G, Giordano C, Guzzo G, Rasola A, et

- al.: Inhibition of Glucose-6-phosphate Dehydrogenase Sensitizes Cisplatin-Resistant Cells to Death. *Oncotarget* 2015; 6(30): 30102-14.
28. Han Y, Kim B, Cho U, Park IS, Kim SI, Dhanasekaran DN, et al.: Mitochondrial Fission Causes Cisplatin Resistance under Hypoxic Conditions via ROS in Ovarian Cancer Cells. *Oncogene* 2019; 38(45): 7089-105.
29. Lee J, Han Y, Kim S, Jo H, Wang W, Cho U, et al.: Mitochondrial Fission Enhances IL-6-Induced Metastatic Potential in Ovarian Cancer via ERK1/2 Activation. *Cancer Sci* 2024; 115(5): 1536-50.
30. Muselli F, Mourgues L, Morcos R, Rochet N, Nebout M, Guerci-Bresler A, et al.: Combination of PKC δ Inhibition with Conventional TKI Treatment to Target CML Models. *Cancers* 2021; 13(7): 1693-710.

GLDC Promotes Cisplatin Resistance of Ovarian Cancer Cells by Enhancing mtROS-Driven Mitochondrial Fission

Do, Thi Yen

Department of Obstetrics and gynecology
Graduate School

Keimyung University

(Supervised by Professor Shin, So Jin)

(Abstract)

Ovarian cancer remains the most lethal gynecological malignancy worldwide, with cisplatin resistance presenting a major obstacle to the effectiveness of current treatment strategies. Glycine decarboxylase (GLDC), a key enzyme involved in glycine metabolism, is linked to tumor initiation and progression. In this study, I investigate the pivotal role of GLDC in ovarian cancer, particularly its function in cisplatin resistance. High GLDC expression is closely associated with poor overall survival in patients with ovarian cancer. Cisplatin-resistant ovarian cancer cells exhibit a higher protein expression level of GLDC compared to their sensitive parental counterparts. Interestingly, I found that GLDC upregulation enhances mitochondrial reactive oxygen species (mtROS) production, whereas knockdown GLDC subsequently reduces significantly

mtROS production using mitoSOX staining. Furthermore, I also observed an increase in dynamin-related protein 1 (DRP1)-mediated mitochondrial fission in cisplatin-resistant ovarian cancer cells compared to parental cells. Knockdown of GLDC-driven mtROS production suppression inhibits mitochondrial fragmentations, thereby sensitizing ovarian cancer cells to cisplatin treatment. Mechanistically, GLDC-induced mtROS stimulates phosphorylation of protein kinase C δ (PKC δ) at Threonine 505, promoting mitochondrial fission in cisplatin-resistant ovarian cancer cells. These findings highlight the potential role of GLDC as a promising therapeutic target to overcome cisplatin resistance in ovarian cancer.

GLDC Promotes Cisplatin Resistance of Ovarian Cancer Cells by Enhancing mtROS-Driven Mitochondrial Fission

도 티 엔

계명대학교 대학원

의학과 산부인과 전공

(지도교수 신 소 진)

(초록)

난소암은 부인암에서 예후가 가장 나쁜 암인데 난소암 치료에 주로 사용되는 cisplatin에 대한 높은 내성이 예후가 나쁜 원인 중 하나로 작용한다. 높은 cisplatin 내성은 난소암 치료에 주요한 장애물로 작용한다. Glycine 대사에 관여하는 핵심 효소인 glycine decarboxylase (GLDC)가 암발생과 관련이 있다는 연구 결과가 최근 보고되고 있다. 따라서 본 연구는 난소암 발생에 관여하는 GLDC의 역할을 조사하고 cisplatin 내성발생에 관여하는 GLDC의 기능을 규명하는 것을 목표로 한다. 높은 GLDC 발현이 난소암 환자들의 낮은 생존율과 연관되어 있는 것을 확인하였다. Cisplatin 내성 난소암 세포는 내성을 나타내지 않는 난소암 세포에 비해 GLDC의 발현이 더 높은 것을 확인하였다. 흥미롭게도 GLDC의 발현 증가가 mitochondrial reactive oxygen species (mtROS) 생성을 촉진하고, 반대로 GLDC 발현 감소는 mtROS 생성을 현저히 감소시켰다. 또한 cisplatin 내성을 나타내지

않는 난소암 세포와 비교하여 cisplatin 내성 난소암 세포에서 dynamin-related protein 1 (DRP1)에 의해서 매개되는 mitochondrial fission (미토콘드리아 분열)이 증가하고 이것은 DRP1에 의해 매개된다는 것을 규명하였다. Knockdown of GLDC 발현 감소에 의해 매개되는 mtROS 생성 감소는 미토콘드리아 분열을 억제하고 난소암 세포의 cisplatin에 대해 감수성을 증가시켰다. 기전적으로, GLDC에 의해 유도된 mtROS는 protein kinase C δ (PKC δ)의 505번 아미노산 Threonine (Thr505)을 phosphorylation (인산화)시켜 cisplatin 내성 난소암 세포에서 미토콘드리아 분열을 촉진한다. 본 연구 결과는 GLDC가 난소암에서 cisplatin 내성을 극복하기 위한 잠재적인 치료 표적제로 작용할 수 있다는 가능성을 제시한다.

□ 저자 약력

1994년 베트남 출생

계명대학교 대학원 의학 석사

계명대학교 의과대학 산부인과학교실 박사학위 대학원생(현)

□ 논문 및 저서

「The FGFR Family Inhibitor AZD4547 Exerts an Antitumor Effect in Ovarian Cancer Cells」 Int J Mol Sci 2021. 10.